Heliyon 10 (2024) e39055

Contents lists available at ScienceDirect

Heliyon

journal homepage: www.cell.com/heliyon

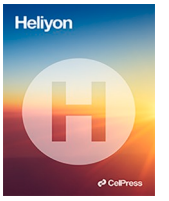

Research article

Comparative metagenomics highlights the habitat-related diversity in taxonomic composition and metabolic potential of deep-sea sediment microbiota

Rui Lu [a,h,1], Denghui Li [a,h,1], Yang Guo [b,i,1], Zhen Cui [a], Zhanfei Wei [a,n], Guangyi Fan [a,c,h], Weijia Zhang [d,j], Yinzhao Wang [e], Ying Gu [c], Mo Han [f,k,l,***], Shanshan Liu [g,j,m,**], Liang Meng [a,h,j,*]

[a] *BGI Research, Qingdao, 266555, China*
[b] *Center of Deep-Sea Research, Institute of Oceanology, Chinese Academy of Sciences, Qingdao, Shandong, 266071, China*
[c] *BGI Research, Shenzhen, 518083, China*
[d] *Institute of Deep-Sea Science and Engineering, Chinese Academy of Sciences, Sanya, 572000, China*
[e] *State Key Laboratory of Microbial Metabolism, International Center for Deep Life Investigation (IC-DLI), School of Life Sciences and Biotechnology, Shanghai Jiao Tong University, Shanghai, China*
[f] *BGI Research, Sanya, 572025, China*
[g] *MGI Tech, Shenzhen, 518083, China*
[h] *Qingdao Key Laboratory of Marine Genomics, BGI Research, Qingdao, Shandong, 266555, China*
[i] *State Key Laboratory of Microbial Technology, Shandong University, Qingdao, Shandong, 266237, China*
[j] *Institution of Deep-Sea Life Sciences, IDSSE-BGI, Sanya, 572000, China*
[k] *Laboratory of Genomics and Molecular Biomedicine, Department of Biology, University of Copenhagen, 2100, Copenhagen, Denmark*
[l] *Shenzhen Key Laboratory of Bioenergy, BGI Research, Shenzhen, 518083, China*
[m] *Shenzhen Key Laboratory of Marine Genomics, BGI Research, Shenzhen, 518083, China*
[n] *National Key Laboratory of Mariculture Biobreeding and Sustainable Goods, Yellow Sea Fisheries Research Institute, Chinese Academy of Fishery Sciences, Nanjing Road 106, Qingdao, 266071, China*

ARTICLE INFO

Keywords:
Marine sediment
Cold seep
Hydrothermal vent
Metagenomics
Metabolic potential

ABSTRACT

Sediment plays a pivotal role in deep-sea ecosystems by providing habitats for a diverse range of microorganisms and facilitates the cycling processes of carbon, sulfur and nitrogen. Beyond the normal seafloor (NS), distinctive geographical features such as cold seeps (CS) and hydrothermal vent (HV) are recognized as life oases harboring highly diverse microbial communities. A global atlas of microorganisms can reveal the notable association between geological processes and microbial colonization. However, a comprehensive understanding of the systematic comparison of microbial communities in sediments across various deep-sea regions worldwide and their contributions to Earth's elemental cycles remains limited. Analyzing metagenomic data from 163 deep-sea sediment samples across 73 locations worldwide revealed that microbial communities in CS sediments exhibited the highest richness and diversity, followed by HV sediments, with NS sediments showing the lowest diversity. The NS sediments were predominantly inhabited by *Nitrosopumilaceae*, a type of ammonia-oxidizing archaea (AOA). In contrast, CSs and HVs were

* Corresponding author.
** Corresponding author.MGI Tech, Shenzhen, 518083, China.
*** Corresponding author.
E-mail addresses: hanmo@genomics.cn (M. Han), liushanshan@mgi-tech.com (S. Liu), mengliang1@genomics.cn (L. Meng).
[1] These authors contributed equally.

https://doi.org/10.1016/j.heliyon.2024.e39055
Received 15 May 2024; Received in revised form 27 September 2024; Accepted 7 October 2024
Available online 9 October 2024

dominated by *ANME-1*, a family of anaerobic methane-oxidizing archaea (ANME), and *Desulfofervidaceae*, a family of sulfate-reducing bacteria (SRB), respectively. Microbial networks were established for each ecosystem to analyze the relationships and interactions among different microorganisms. Additionally, we analyzed the metabolic patterns of microbial communities in different deep-sea sediments. Despite variations in carbon fixation pathways in ecosystems with different oxygen concentrations, carbon metabolism remains the predominant biogeochemical cycle in deep-sea sediments. Benthic ecosystems exhibit distinct microbial potentials for sulfate reduction, both assimilatory and dissimilatory sulfate reduction (ASR and DSR), in response to different environmental conditions. The presence of nitrogen-fixing microorganisms in CS sediments may influence the global nitrogen balance. In this study, the significant differences in the taxonomic composition and functional potential of microbial communities inhabiting various deep-sea environments were investigated. Our findings emphasize the importance of conducting comparative studies on ecosystems to reveal the complex interrelationships between marine sediments and global biogeochemical cycles.

1. Introduction

The deep-sea benthic ecosystem plays a crucial role in maintaining the overall health and functioning of marine environments [1–3]. Despite the harsh conditions, deep-sea sediments host diverse and unique communities of organisms that have adapted to survive in these challenging environments [4,5]. In addition to normal seafloor ecosystems, cold seeps and hydrothermal vents are two distinct ecosystems [6–8]. Cold seeps are characterized by fluid emissions containing hydrocarbons and hydrogen sulfide, with temperatures akin to seawater [8–11]. Within cold seep ecosystems, there are primarily two types of microorganisms, anaerobic methane-oxidizing and sulfate-reducing microorganisms, that play crucial roles in the degradation and recycling of organic matter, contributing to overall carbon and energy cycling in these ecosystems [10,12–16]. In contrast to cold seeps, hydrothermal vents typically contain water rich in sulfide and metals, with temperatures ranging from 2 °C to 400 °C [17]. Hydrothermal vent ecosystems are predominantly situated at spreading centers on the seafloor, arising from hydrothermal vent within the Earth's crust [7]. Chemosynthetic bacteria and archaea constitute the primary trophic level within hydrothermal vent ecosystems, serving as the cornerstone of these unique ecosystems by converting inorganic carbon into organic biomass through chemosynthesis [18,19].

Previous research has demonstrated that hydrothermal vent and cold seep habitats exhibit similar community structures, yet they also harbor habitat-specific species [20,21]. Moreover, the most notable disparities in communities across different seafloor ecosystems occur within hydrothermal vent habitats and cold seep habitats, and the significant presence of endemic species can be found in both ecosystems [22]. For instance, at the phylum taxonomic level, both hydrothermal vents and cold seeps contain a considerable proportion of common phyla, including *Chloroflexi*, *Proteobacteria*, *Crenarchaeota* and *Thaumarchaeota*, irrespective of whether bacteria or archaea are considered [23–26]. However, at more detailed taxonomic level, such as the genus and species levels, the number of shared genera and species is limited. This may be related to variations in the fluid composition of the two ecosystems, in conjunction with differences in their discharge volumes and rates of organic deposition [20,27,28]. These differences in chemical compositions not only influence the distribution of microbial communities capable of utilizing specific compounds but also affect their adhesion and metabolic activities [20].

Although deep-sea hydrothermal vents and cold seeps are all sunlight-independent and chemosynthetic ecosystems, microbial metabolism in hydrothermal vent and cold seep ecosystems exhibits significant differences. In cold seep ecosystems, microbial metabolism predominantly hinges on the anaerobic oxidation of methane [29]. Conversely, in hydrothermal ecosystems, microbial metabolism is more reliant on the oxidation of inorganic substances such as hydrogen sulfide and hydrogen [30]. Within cold seep ecosystems, *ANME* archaea can transform methane into inorganic carbon and also generate organic carbon, such as acetic acid. This provides a carbon source for heterotrophic microbes within the ecosystem, significantly impacting deep-sea carbon cycling and global climate change [29]. Within hydrothermal vent ecosystems, the sulfide cycle is one of the most prominent biogeochemical cycles. Microbes in hydrothermal vent ecosystems primarily derive energy through the oxidation of sulfides and reduction of metals [31]. For example, some hyperthermophiles like *Pyrococcus yayanosii* utilize hydrogen sulfide and oxygen for metabolism under high temperature and pressure conditions [32]. Additionally, existing literature has reported a series of other biogeochemical element cycles in these ecosystems, such as the rTCA cycle and nitrogen fixation pathways in cold seeps, and the nitrogen cycle in hydrothermal vents [33–35]. Despite the burgeoning interest in the biogeochemical processes within cold seep and hydrothermal vent ecosystems, the majority of research has been confined to localized sites or limited regional samples, and focusing on specific metabolic pathways. To date, there is a notable absence of extensive global comparative analyses that amalgamate data from various cold seep and hydrothermal vent habitats. Such comparative studies are essential for elucidating the broader ecological and biogeochemical implications of these unique marine environments.

In this study, we gathered a total of 163 metagenomic datasets from normal ecosystems, cold seeps, and hydrothermal vents across the globe. After assembling and binning, we constructed a catalog consisting of 3048 species-level genome bins (SGBs). The primary objective of this analysis was to investigate the composition, diversity, and metabolic potential of microbial communities within the three ecosystems. Additionally, we established correlations between microbial taxa and metabolic potential while predicting the metabolic patterns of microbial communities in different geographic regions of deep-sea sediments. Specifically, we analyzed metagenomes from three distinct ecosystems to address the following questions: (i) identify the predominant and frequently occurring

microbial groups in deep-sea sediments; (ii) evaluate the influence of environmental factors on the organization principles of microbial community structure and function in deep-sea sediments; (iii) discover distinctive indicators in various ecosystems; and (iv) explore potential variations in the contribution of microbial community metabolism to biogeochemical cycling across different ecosystems.

2. Results

2.1. A worldwide deep-sea sedimentary metagenomic dataset reveals unexplored microbial diversity

Metagenomic sequencing data from 163 deep-sea sediment samples were obtained for further analyses; these samples included NS sediments (n = 35), CS sediments (n = 71), and HV sediments (n = 57) (Fig. 1a and b). Among them, 108 metagenomes were derived from published articles, while the other 55 were newly collected from the Haima and Site F cold seeps in the South China Sea (Supplementary Table S1). The samples exhibited a wide distribution of locations worldwide, ranging in depth from 1000 m to 9177 m. *De novo* assembling and binning generated 3048 non-redundant draft genomes (>50 % completeness and <10 % contamination), 581 of which were high-quality SGBs (>90 % completeness and <5 % contamination) (Supplementary Table S2). The quality-controlled reads from the 163 metagenomes exhibited a high mapping ratio to all SGBs (average 49.20 %), indicating a comprehensive representation of the SGBs in the recovered microbiomes (Fig. S1).

The 3048 SGBs were distributed across three different environments: NS (354), CS (1,086), and HV (1,608) (Fig. 1c). Classification of these SGBs using the Genome Taxonomy Database (release 202) revealed 684 archaeal and 2364 bacterial SGBs, representing 3048

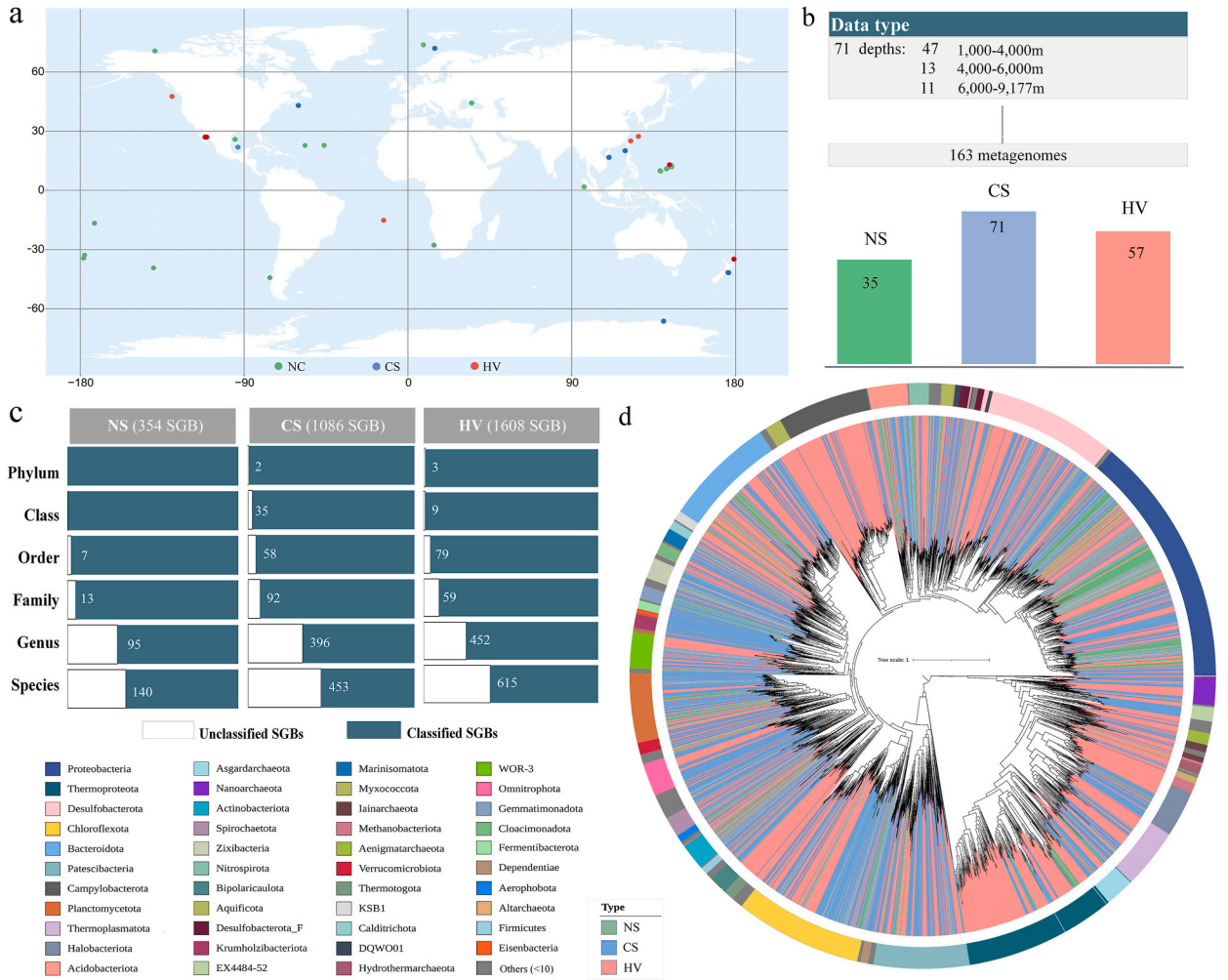

Fig. 1. The characterization of deep-sea sediment samples and metagenome-assembled genomes catalog. Normal seafloor, NS; cold seep, CS; hydrothermal Vent, HV. (a) Geographic distribution and types of 163 deep-sea samples, on the basis of published information. (b) Depth breakdown of the samples used in this study. Sample and data contributions by projects in this program, including the NS, CS and HV sediments. (c) Total MAGs unclassified by GTDB-Tk at each taxonomic level. (d) Phylogenetic genome tree showing the diversity and environmental source of the recovered species.

prokaryotic species affiliated with 19 archaeal and 91 bacterial phyla (Fig. S2). Most of the SGBs (85.56 %) were annotated as novel species, while five of the SGBs obtained from the CS and HV sediments were assigned to novel phyla (Fig. 1c). The predominant phyla from which these SGBs were derived consisted of *Proteobacteria* (n = 422), *Desulfobacterota* (n = 225), *Chloroflexota* (n = 214), *Bacteroidota* (n = 188), and *Patescibacteria* (n = 160) for bacteria, and *Thermoproteota* (n = 254), *Thermoplasmatota* (n = 103), *Halobacteriota* (n = 77), *Asgardarchaeota* (n = 50), and *Nanoarchaeota* (n = 48) for archaea (Fig. 1d and Fig. S2).

2.2. Comparisons of the microbiomes of NS, CS and HV sediments reveal habitat-related differences in diversity

(i) **Taxonomic composition and dominant phylotypes.** The dominant phylotypes comprised highly abundant (ranking in the top 10 % of the most common phylotypes, sorted by their percentage of SGBs) and ubiquitous (present in over half of the 163 marine sediment samples) populations. Not surprisingly, our global marine dataset included microbiome communities that were highly variable with respect to their diversity and overall composition. We observed that only five dominant phyla, *Acidobacteriota*, *Thermoproteota*, *Chloroflexota*, *Proteobacteria* and *Bacteroidota*, exhibited global dispersion (Fig. S3). In the NS sediment samples, the prevailing phyla identified were *Proteobacteria* and *Thermophiles*. Contrastingly, in the CS sediment samples, *Halobacteria*, *Desulfobacteria*, and *Chloroflexi* constituted the predominant phyla. As for the HV sediment samples, *Thermophiles*, *Campylobacteria*, and *Desulfobacteria* were the principal phyla detected. (Fig. S4). Additionally, we selected the top 30 SGBs in terms of mean coverage from each environment for abundance clustering, aiming to reveal differences in taxonomic composition between different habitats (Fig. 2a). In the NS sediment, SGBs assigned to *Nitrosopumilaceae*, which included SGB70, SGB85, and SGB72, were highly abundant. In CS, the highly abundant SGBs were assigned to the *ANME-1* family, which included SGB03, SGB47, and SGB53. In the HV population, the highly abundant SGBs were annotated as the family *Desulfofervidaceae*, which included SGB02 and SGB06 (Fig. 2a). **(ii) Microbial diversity in marine sediment.** We further analyzed the overall differences in taxonomic compositions among the three habitats. By calculating the richness, Chao1, Shannon, and Simpson indices for all samples, we utilized analysis of variance (ANOVA) to evaluate the statistical significance of differences between the samples. Significant differences in the alpha diversity indices were found among sediments from the different ecosystems (Kruskal-Wallis test, $p < 0.001$). The highest Chao1 and Shannon indices were observed in the CS sediments, while the lowest were in the NS sediments (Fig. 2b). These findings indicated that the richness and diversity of the sediment microbial communities are greater in CSs than in NSs. In addition to the differences in alpha diversity, the beta diversity of the microbial

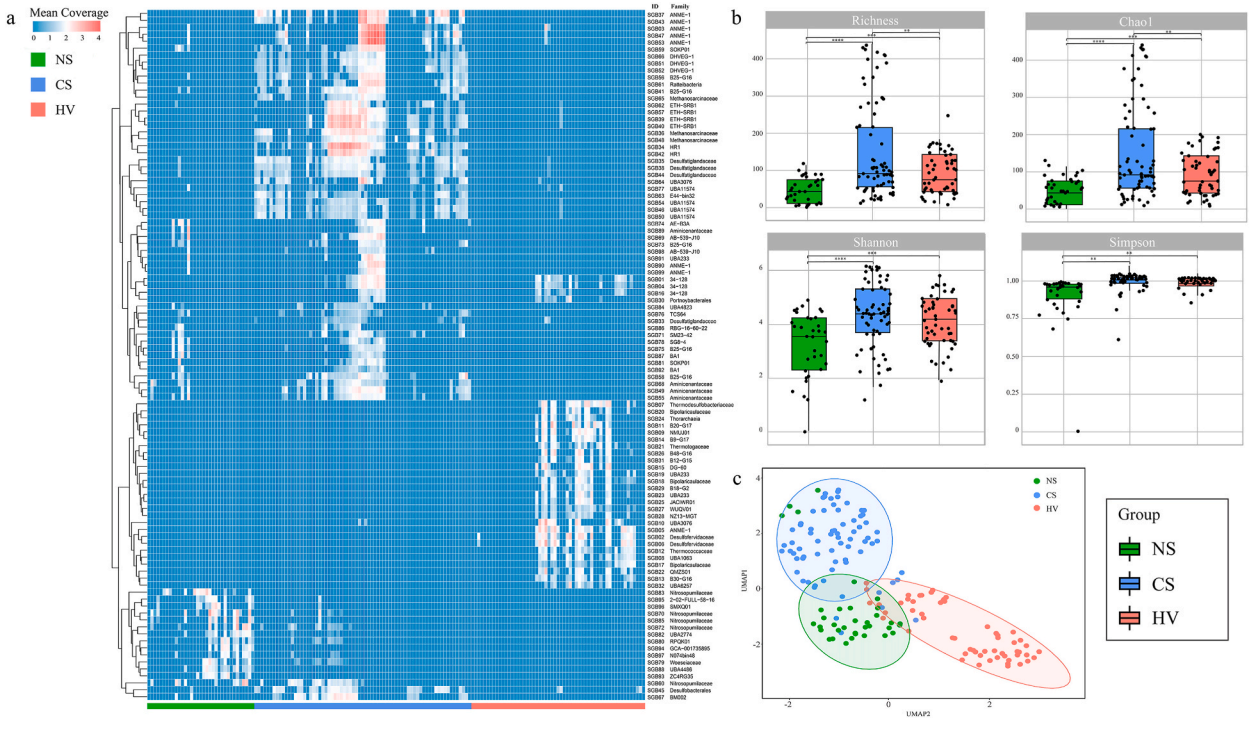

Fig. 2. The relative abundances and diversity of dominant microbial family in sediments of NS, CS, and HV groups. (a) Heat map with taxonomic information on the dominant species (the top 33 SGB of relative abundance in each habitat) in 163 samples. Red tint indicates a higher relative abundance. (b) Differences in alpha diversity metrics both in the NS, CS and HV (linear model on Richness, Chao1, Shannon and Simpson index, $p \leq 0.001$). (c) UMAP dimensionality reduction plots generated using the Bray–Curtis dissimilarity index values derived from the SGBS populations. (For interpretation of the references to colour in this figure legend, the reader is referred to the Web version of this article.)

communities was also significantly affected by the habitat. Using the overall relative abundance profile of SGBs, the uniform manifold approximation and projection (UMAP) approach revealed obvious differences between habitats (Fig. 2c).

2.3. Co-occurrence network analysis reveals diverse patterns of intertaxon correlation in different deep-sea habitats

By performing a co-occurrence network analysis considering the non-random aggregation patterns of microbial communities in marine sediments from different habitat types, we established three network interfaces with the top 200 SGBs from each habitat to better determine the topological and taxonomic characteristics of the marine microbial co-occurrence patterns (Fig. 3 and Supplementary Table S1). According to the results, 1887 edges (NS = 569, CS = 1,011, and HV = 307) were captured among the 440 nodes (NS = 137, CS = 164, and HV = 139) that exhibited significant correlations between species ($\rho > 0.8$, $P < 0.05$). Moreover, significant topological characteristics were derived to determine the complex patterns of interrelationships among nodes. When the nodes in the NS network were modularized, they were divided into 17 main modules (Fig. 3). Each module consisted of a set of SGB nodes with more frequent interconnections within the module than between modules. In addition, the nodes were divided into 74 families (Fig. 3). Among them, *Nitrosopumilaceae*, *Woeseiaceae*, *Alteromonadaceae*, *Flavobacteriaceae*, *Flavobacteriaceae* and *Enterobacteriaceae* accounted for 26.84 % of all nodes, and they were also dominant families in the community. In contrast, the six keystone families with the highest numbers of CS were *AB-539-J10*, *ANME-1*, *ETH-SRB1*, *ANME-2c*, *HR1* and *DHVEG-1*. The most important groups in the HV network were *Sulfurimonadaceae*, *Acidilobaceae*, *UBA6429*, *Thiomicrospiraceae*, *Thiomicrospiraceae* and *Bipolaricaulaceae*. Additionally, the degrees of change in the *Thalassarchaeota* family in the NS, *UBA3072* in the CS, and *SZUA-152* in the HV were 25, 37 and 22, respectively. These represent high and low betweenness centrality values, indicating that these species can be considered central species in their respective habitats.

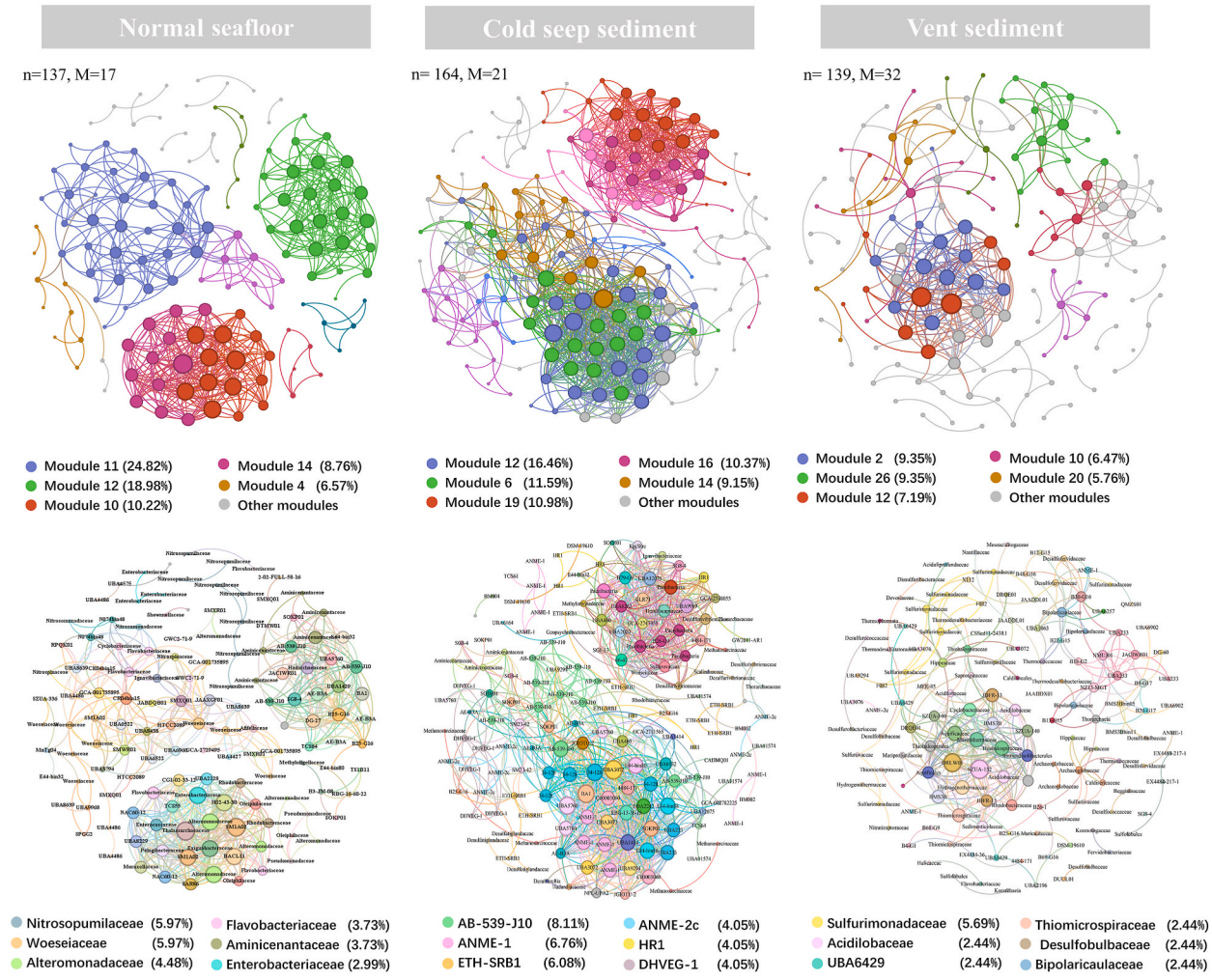

Fig. 3. The co-occurrence patterns under NS, CS and HV sediments revealed by network analysis at the family level. Node composition of the main modules at the family level in the NS, CS and HV microbial co-occurrence network. Connection stands for a significant correlation between species ($\rho > 0.8$, P-value <0.05). The size of each node is proportional to the number of connections.

The microbial networks under NS, CS and HV exhibited differences based on significant topological characteristics (Fig. 3). The average clustering coefficient and the average degree of the network under CS were 0.572 and 12.329, respectively (Table 1). These results indicate that the network has a greater correlation under CS than under NS, and both are significantly greater than those under HV. This suggests that microbial taxa in CS associate more closely with each other. Interestingly, compared to those in cold seep ecosystems, the topological characteristics of the microbial network under hydrothermal vents are markedly different. The HV network had a clustering coefficient of 0.006, suggesting that most of the SGBs have few connections with their neighborhood (Table 1). Despite the low average clustering coefficient, the HV network has a high modularity value of 0.843, indicating approximately 32 communities within the network. Microbial communities from HVs form smaller clusters, while those in CS and NS are more interconnected SGBs. Finally, the eigenvector centrality in the HV network is very low at 0.006, indicating rare interactions between SGBs and central SGBs in the community. This suggests that microbial communities under HV conditions have less centralization and fewer interactions compared to those in CS and NS.

2.4. Metabolic reconstruction

To better understand the role of deep-sea sediment microorganisms, we predicted and annotated their protein-coding genes from 3048 SGBs using the KEGG database. We subsequently reconstructed the major metabolic potential of these SGBs and further revealed their relationships with habitats (Fig. 4).

Microorganisms may assimilate CO_2 through different mechanisms. Indeed, a total of six CO_2 fixation pathways, including the reductive citrate cycle (rTCA), dicarboxylate-hydroxybutyrate cycle (3DC/4-HB), reductive pentose phosphate cycle (Calvin), 3-hydroxypropionate bicycle (3-HP), 3-hydroxypropionate/4-hydroxybutyrate (3-HP/4-HB), and reductive acetyl-CoA pathway (Wood–Ljungdahl pathway, WL), were found in nature. Among the functional genes related to carbon fixation, key enzymes like *ppc* (from the 3DC/4HB pathway) and *accA* (from the 3HP/4HB pathway) were most abundant, indicating that they are the primary pathway of microbial CO_2 fixation in deep-sea sediments. Notably, we also observed that the genes encoding key enzymes of these pathways exhibited habitat-related patterns in terms of relative abundance. The microbial communities in the NSs primarily functioned via the 3DC/4HB, 3-HP/4-HB, and rTCA pathways. Moreover, the CS and HV sediments exhibited greater abundances of *aclA/B* and *acsB*, while *cooS* was observed to have the highest relative abundance in the HV. These findings suggest that in addition to the aforementioned pathways, the WL pathway was also dominant in the CS and HV sediments (Fig. 4).

Microbes may also play a crucial role in the cycling of sulfur. There are four microbial sulfur metabolic pathway categories: sulfur reduction, sulfur oxidation, assimilation of inorganic sulfur compounds, and mineralization of organic sulfur compounds. We noticed that *sat*, which encodes ATP sulfurylase and plays a crucial role in the reduction of SO_4^{2-}, was the most abundant gene related to sulfur metabolism (Fig. 4). As there were two pathways for sulfate reduction, dissimilatory sulfate reduction and assimilatory sulfate reduction. The key enzymes *dsrA* (from the dissimilatory sulfate reduction) were most abundant in the CS and HV sediments, and the key enzymes *sir* (from the assimilatory sulfate reduction) were most abundant in the NS sediments. Additionally, two other genes related to the assimilatory sulfate pathway, *cysC* and *cysH*, also exhibited higher relative abundances in NS sediments.

Although the relative abundances of genes related to nitrogen utilization may not be as high as those involved in carbon fixation and sulfur metabolism, the deep-sea sediment microbiome exhibits comprehensive potential for nitrogen utilization. (Fig. 4). Among the marker genes of nitrogen-fixing microorganisms, *nifH* exhibited the highest relative abundance in CS sediments, followed by HV sediments (Fig. 4 and Fig. S5). Moreover, in the NS sediments, the relative abundances of genes related to N_2O production by denitrification were greater than those related to N_2O utilization. Additionally, the nitrite in the HV sediments was mainly used to produce ammonia through ammonia monooxygenase (*amoA*). Conversely, in the NS and CS sediments, the dominant process involved the synthesis of nitrite through the utilization of ammonia by hydroxylamine reductase (*hcp*).

In addition, we established a link between microorganisms and functional metabolism. Our findings revealed that distinct ecological environments exhibit variations in microbial taxa participating in identical biogeochemical cycles. Specifically, we identified 88 phyla implicated in carbon cycling in CS sediment and 83 phyla in HV sediment. In contrast, carbon cycling in the NS sediments involved only 43 phyla. Furthermore, the CS and HV sediments also exhibited more functional microbial phyla associated with sulfur, nitrogen, and methane cycling than did the NS sediment (Fig. 5).

3. Discussion

Previously, microbial communities in marine sediments were classified as aerobic or anaerobic ecosystems based on the analysis of microbial diversity in 299 sediment samples collected from various locations worldwide [36]. Another study categorized marine sediments according to their environmental characteristics by comparing the microbial diversity among shallow marine sediments,

Table 1
Properties of the correlation-based network.

Env[a]	NO. of Edges	NO. of Nodes	Modularity	Average clustering coefficient	Average degree	Density	Eigenvector centrality	Diamete
NS	569	137	0.732	0.537	8.307	0.061	0.021	11
CS	1011	164	0.722	0.572	12.329	0.076	0.019	11
HV	307	139	0.843	0.381	4.417	0.032	0.006	10

[a] Env, Environment; NS, Normal seafloor; CS, Cold seep; HV, Hydrothermal vent.

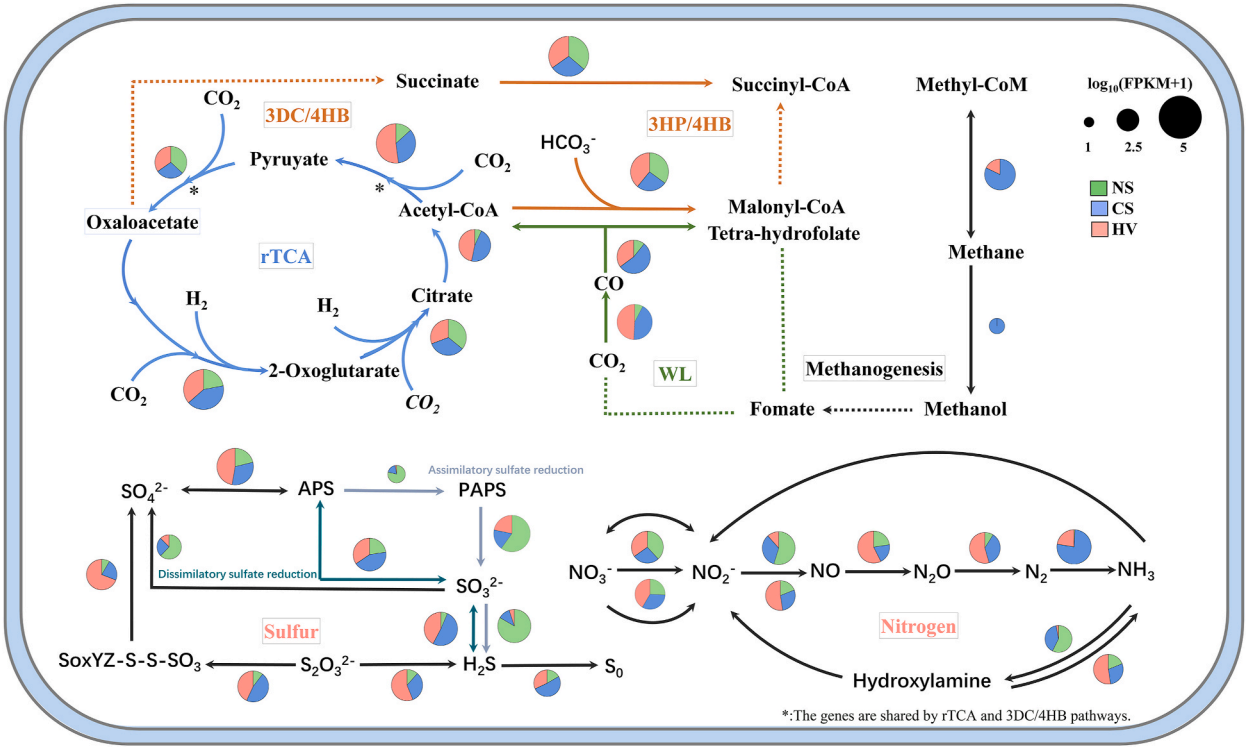

Fig. 4. The patterns of genes related to carbon, nitrogen, and sulfur cycling in sediments from NS, CS, and HV groups. Microbial taxa contribution to the abundance of genes in each of the three ecosystem groups. The circular size represents the FPKM average value of the gene after standardization in all samples.

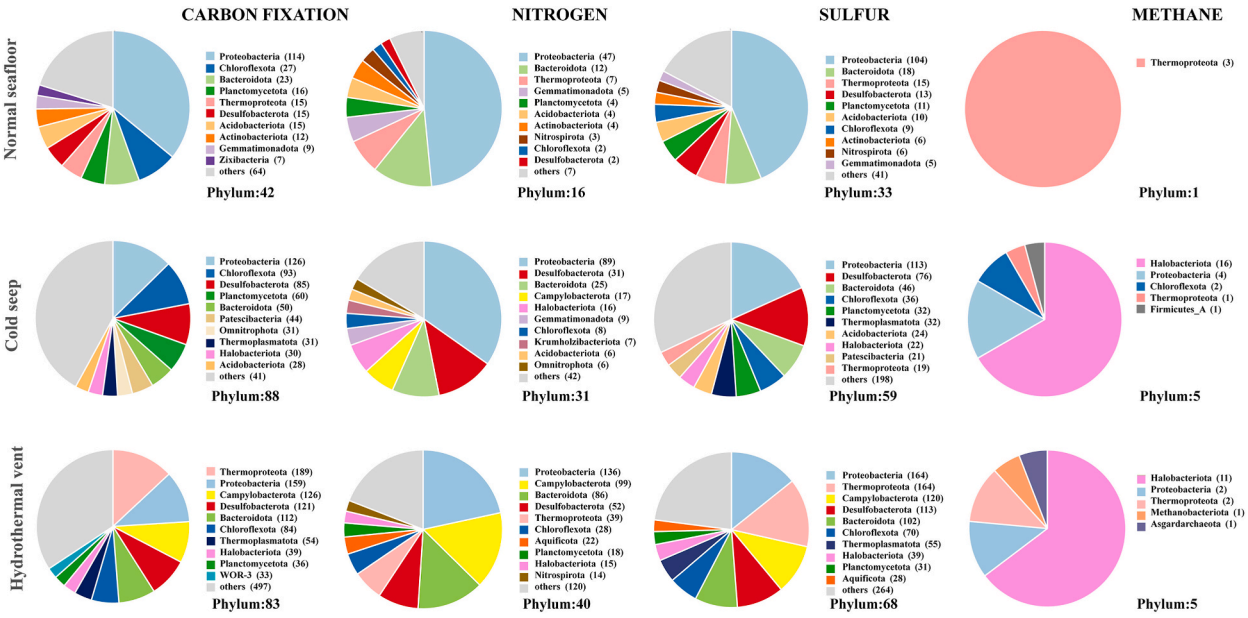

Fig. 5. The microbial taxonomic composition involved in the cycling of carbon, nitrogen, sulfur and methane in three benthic ecosystems.

cold seeps, and hydrothermal vent habitats [22]. Cold seep communities were found to have moderate microbial richness and unique bacterial and archaeal groups that are widely distributed, compared to other marine ecosystems [22]. While these studies have provided valuable insights, they have certain limitations, primarily due to their reliance on amplifying 16S rRNA gene sequences. However, the emergence of high-throughput sequencing technologies, such as metagenomic sequencing, has addressed these

limitations by providing information on potential metabolic functions in addition to microbial community composition [37]. In contrast to these prior researches, our study not only offers a systematic comparison of deep-sea sediments based on geographical attributes but also employs metagenomic data to precisely determine the correlation between microbial composition and ecological functions. This approach sheds light on the complex interactions within these environments.

Based on the taxonomic profiles of 3048 SGBs, our analysis revealed that only five phyla demonstrated global dispersion. Although this discovery was unexpected, it could be explained by sampling strategies or sequencing depth. Despite their limited representation, these phyla collectively accounted for an average relative abundance of 35.21 % and 30.72 % in the CS and HV ecosystems, respectively. Additionally, these taxa constituted more than half of the microbial communities in the NS (Fig. S4). It is suggested that the majority of microbial phylotypes are infrequent, with only a limited number being prevalent, while many of these infrequent phylotypes show a widespread distribution throughout marine sediments. Moreover, ANME and SRB were identified as the highly abundant populations within CS and HV, respectively. A previous study revealed that the dominant microorganisms in sediments at a depth of 390 m in Storfjordrenna seeps was ANME/Seep-SRB1 [38], which aligns with our findings. It can be speculated that microbial phylotypes and particular habitats are inevitably related. However, further investigations are needed to determine the ecological roles and functions of these highly abundant populations and their interactions with the less abundant phylotypes in marine sediments.

Furthermore, we observed significant differences in microbial community diversity among the sediments within the NS, CS, and HV environments. The distinct community compositions, as indicated by inter-sample similarities in SGB composition, suggest a greater level of diversity among marine sediment environments. This elevated diversity is likely influenced primarily by local geochemistry, specifically by the concentrations of methane, sulfide, nitrate, and other substances, rather than by the geological environment or random diffusion events [39–41]. Notably, our findings align with recent studies that have reported the highest microbial species diversity at cold seep sites [22,33,42,43]. This could be attributed to the local heterogeneity of the sampling infiltration system, which potentially affects the availability of ecological niches for microbial colonizers. An unexpected finding was the microbial communities within the HV ecosystem exhibit a lower degree of network connectivity in comparison to those in the NS and CS ecosystems. Prior research has shown that, in contrast to cold seeps, hydrothermal vents support a greater variety and abundance of metal ions and hydrogen gas, which can serve as sources of nutrition for many microorganisms [44]. Despite the absence of metal ions and physicochemical parameters such as hydrogen, we propose that this outcome may be ascribed to a more varied growth strategy of microorganisms in nutrient-abundant hydrothermal vent ecosystems, rather than solely depending on microbial interactions.

The biogeochemical cycle in marine sediments and the control of organic matter as a dynamic repository are driven by intricate interactions between microbial communities and geochemical processes [45]. Previous studies have indicated that the cycling of active substances in sediments involving microbes includes carbon fixation, sulfate reduction and sulfide oxidation, nitrogen fixation, and ammonia oxidation, among others [21,46–48]. Another study further revealed that microorganisms residing in deep-sea sediments have diverse potential roles in the biogeochemical cycle, which are highly related to their habitats [49]. Although the metabolic potential of most carbon fixation pathways was similar, the WL pathway was found to be enriched in the CS and HV sediment microbiota. Furthermore, our findings suggest that while sulfate reduction is the predominant sulfur metabolism pathway in deep-sea sediments, different habitats exhibit distinct preferences for dissimilatory and assimilatory pathways. Additionally, our study indicates a discrepancy in the metabolic potential for the greenhouse gas N_2O production and utilization within the NS sediments, highlighting an accumulation of N_2O-producing capabilities without a corresponding increase in N_2O-consuming pathways. This could be a significant factor in climate change, particularly considering the vast expansion of normal deep-sea beds.

Further investigations into the relationship between the metabolic preference of the deep-sea microbial community and its adaptation to specific habitats could significantly contribute to our understanding of the ecological importance of the deep-sea microbiota. We discovered that the CS sediment had a greater abundance of *nifH* than the NS and HV sediments. These findings support previous research conducted by Dong et al., who analyzed global metagenomic data from 11 cold seep sites and identified a wide range of nitrogen-rich organisms with diverse phylogenetic and metabolic decomposition patterns [33]. These nitrogen-rich organisms in CS sediments likely play a crucial role in maintaining the global nitrogen balance. Furthermore, our study revealed that despite differences in microbial community composition, genome size and physiological characteristics, microorganisms in diverse ecosystems exhibit similar metabolic capabilities [50]. This observation is consistent with our findings that functional microorganism diversity varies across habitats, but all of these microorganisms play pivotal roles in the cycling of carbon, nitrogen, and sulfur. However, we also observed that microorganisms in different environments have distinct metabolic contributions when faced with significant geochemical disparities.

4. Conclusions

In conclusion, our research utilized deep-sea sediment metagenomic data collected from worldwide locations to study microbial diversity and biogeochemical processes across different benthic ecosystems in the deep sea. The analysis of the microbial genomic catalog allowed us to identify the global dispersal and dominant microbial phylotypes present in different deep-sea sedimentary ecosystems. Specifically, the NS sediments are primarily composed of AOA, whereas ANME and SRB predominate in CS and HV sediments, respectively. Understanding microbial interaction patterns provides insights into the intricate ecological dynamics within these benthic ecosystems. Notably, the complexity of the biogeochemistry of HV sediments is underscored by the limited observed microbial interactions in this environment. Furthermore, the metabolic potentials of microbial communities in deep-sea sediments play diverse and important roles in biogeochemical cycles, including carbon fixation, sulfur compound reduction and oxidation, nitrogen fixation, and greenhouse gas production. The ecological functions of these metabolic pathways differ among habitats. Further examination revealed that the 3DC/4-HB and 3-HP/4-HB pathways of carbon fixation, along with the assimilatory sulfate-reducing

pathway, were more abundant in NS sediments. In contrast, the rTCA and WL pathways of carbon fixation and the dissimilatory sulfate-reducing pathway were dominant in CS and HV sediments. Additionally, the presence of nitrogen-fixing organisms in CS sediments may significantly influence global nitrogen balance, alongside methane oxidation. These distinct pathways are integral to marine biogeochemical cycles. Overall, this research highlights the importance of microbial communities in deep-sea sediments for the biogeochemical cycles and ecological dynamics of different benthic ecosystems. Understanding the specific metabolic pathways and interactions within these communities is crucial for comprehending the complex processes occurring in the deep sea.

5. Materials and methods

5.1. Sample collection

A total of 163 deep-sea metagenomes were utilized in the present study. Among these, 108 datasets were sourced from the National Center for Biotechnology Information (NCBI) website. The selection criteria for these datasets involved filtering based on information provided in the respective papers or NCBI metadata. Specifically, only metagenomes collected from oceanic regions at depths exceeding 1000 m and sequenced using metagenomic paired-end libraries were considered for inclusion (Table S1). These 108 samples were then categorized into three ecosystem groups based on the sampling information (Table S1). Furthermore, 35 samples were assigned to normal sediment, 16 samples to cold seep ecosystems, and 57 samples to hydrothermal vent ecosystems. Since the number of published samples collected from cold seep ecosystems were limited, we additionally integrated 55 samples from related projects. Out of the 55 cold seep samples from the South China Sea, 19 were collected from the "Site F″ cold seep in a related project, and their metagenomic data have already been published. The remaining 36 cold seep samples were newly collected from the "Haima" cold seep and sequenced in this study.

5.2. DNA extraction and sequencing

A modified SDS-based DNA extraction method was applied to extract DNA from the 36 sedimentary samples collected from the "Haima" cold seep [51]. The extracted microbial DNA was fragmented to achieve a size range of 500–800 bp using a Covaris E220. Fragments between 150 bp and 250 bp were selected using AMPure XP beads (Agencourt, Beverly, MA, USA). T4 DNA polymerase (Enzymatics, Beverly, MA, USA) was utilized to repair the DNA fragments, resulting in blunt ends, which were further modified at the 3′ ends to obtain sticky dATP ends. These DNA fragments were then ligated with T-tailed adapters at both ends and amplified for eight cycles. Subsequently, a single-strand circularization process was performed to generate a single-strand circular DNA library. The libraries were subsequently sequenced on the DNBSEQ-T1 platform using a paired-end 100 bp sequencing strategy.

5.3. Assembly and genome binning

All the raw reads were quality controlled using SOAPnuke (v 1.5.2) with the parameters (-l 20 -q 0.2 -n 0.05 -Q 2 -d -c 0–5 0-7 1) to remove low-quality, adapter-contaminated and duplication reads [52]. The filtered reads were assembled with MEGAHIT (v 1.1-beta) with the parameters –min-count 2/3 –k-min 33 –k-max 53 –k-step 10 –no-mercy and filtered out scaffold/contig whose length was less than 300 bp [53]. Contigs longer than 300 bp from all the metagenomic data were utilized to create bins via three alternative binning algorithms of the '–metabat2 –maxbin2 –concoct' MetaWrap workflow (v 1.1.5) [54]. The outputs of the three algorithms were subsequently combined using the bin_refinement module in the metaWRAP process. Filtered bins were collected and clustered using dRep (v 3.2.2) at 95 % identity, and the highest quality genome with a completeness greater than 50 % and a contamination lower than 10 % of each cluster was collected as the species-level genome bins (SGBs) set used in this study [55]. Then, taxonomic annotation of the SGBs was carried out by GTDB-TK (v 1.6.0) [56]. Clean reads from two libraries of each sample were concatenated and SGBs were constructed with Bowtie2 (v 2.5.0) [57]for CoverM (v 0.6.1) (https://github.com/wwood/CoverM) to calculate the relative abundance of the SGBs within the "-m relative_abundance mean covered_fraction" package.

5.4. Phylogenetic analyses

The construction of a phylogenetic tree is a method that aims to determine the evolutionary status of species in a more objective and precise manner. To accomplish this, the genomes were subsequently analyzed using CheckM (v 1.1.2) in combination with the sorted genomes [58]. Concatenated sequences composed of 43 well-aligned conserved proteins were extracted. To eliminate unaligned regions, trimAl (v 1.4) was used [59]. The phylogenetic tree was subsequently constructed using IQ-TREE (v 1.6.10) with the maximum likelihood algorithm (ML) [60]. The best-fit model "LG + F + R10" was selected, and a bootstrap value of 1000 was applied. The constructed phylogenetic tree of conserved proteins evolving at the genome level served to further validate the classification and evolutionary status of the obtained SGBs.

5.5. Diversity and network analyses

Diversity analyses were conducted using the online MicrobiomeAnalyst (http://www.microbiomeanalyst.ca/). The analyses were conducted at species diversity (q value) of 1, that take into accounts the relative abundances of the SGBs and considers various aspects of diversity. The matrix outputted the co-occurrence correlation of the SGBs, where a positive matrix represented a positive correlation

and a negative value represented a negative interaction. The matrix values were entered into Gephi (v 0.10.1) to generate a network of microbial communities, utilizing the built-in diversity feature [61].

5.6. Genes annotations and abundance profiling

Predicting open reading frames (ORFs) of genomic sequences is performed by utilizing Prodigal (v 2.6.2), followed by the annotation of the predicted protein sequences against the KEGG database [62]. Then, the predicted proteins were clustered using the CD-HIT (v 4.8.1) software in order to generate a non-redundant (NR) gene catalog [63]. The predicted genes were annotated by comparing them to the KEGG database using kofamscan (v 1.1.0) [64]. The SGBs were assessed for the completeness of specific pathways and functions based on the canonical pathways available in the KEGG pathway database (https://www.kegg.jp/). The metagenomic relative abundance of genes from SGBs were calculated as the FPKM value by CoverM (v 0.6.1) with params "-m length count".

CRediT authorship contribution statement

Rui Lu: Writing – original draft, Visualization, Methodology, Formal analysis, Data curation, Conceptualization. **Denghui Li:** Writing – original draft, Formal analysis, Data curation, Conceptualization. **Yang Guo:** Formal analysis, Data curation, Conceptualization. **Zhen Cui:** Data curation. **Zhanfei Wei:** Formal analysis, Conceptualization. **Guangyi Fan:** Supervision. **Weijia Zhang:** Supervision. **Yinzhao Wang:** Supervision. **Ying Gu:** Supervision, Resources. **Mo Han:** Writing – original draft, Conceptualization. **Shanshan Liu:** Supervision, Resources. **Liang Meng:** Writing – original draft, Conceptualization.

Data availability statement

Metagenomic data have been submitted to the China National GenBank Sequence Archive (CNSA, https://db.cngb.org/cnsa/) of the China National GenBank Database (CNGBdb) with the project CNP0004691. Accession numbers can be found in the additional Table S1.

Funding

This work was financially supported by the Major Scientific and Technological Projects of Hainan Province (ZDKJ2021028), the National Key R&D Program of China (Grand Nos. 2022YFC2805404 and 2021YFC2800403), the State Key Laboratory of Microbial Technology Open Projects Fund (Project NO. M2023-10), and the Technological Innovation Projects of Qingdao West Coast New Area (Project NO. ZDKC-2022-03).

Declaration of competing interest

The authors declare that they have no known competing financial interests or personal relationships that could have appeared to influence the work reported in this paper.

Acknowledgments

We would like to express our sincerest gratitude to the crews on R/V *Tansuoyihao* and *Kexue* for their professional service. We thank Nannan Zhang, Mingming Yang, Aijun Jiang, Qianyue Ji, Chongyang Cai for their generous assistance. We also appreciate the technical support from China National GeneBank for the library construction and sequencing in whole-genome short reads.

List of abbreviations

NS	normal seafloor
CS	cold seep
HV	hydrothermal vent
AOA	ammonia-oxidizing archaea
ANME	anaerobic methane-oxidizing archaea
SRB	sulfate-reducing bacteria
SGB	species-level genome bin

Appendix A. Supplementary data

Supplementary data to this article can be found online at https://doi.org/10.1016/j.heliyon.2024.e39055.

References

[1] P.V. Snelgrove, The importance of marine sediment biodiversity in ecosystem processes, Ambio (1997) 578–583.
[2] P.V. Snelgrove, Getting to the bottom of marine biodiversity: sedimentary habitats: ocean bottoms are the most widespread habitat on earth and support high biodiversity and key ecosystem services, Bioscience 49 (2) (1999) 129–138.
[3] G. Birch, Determination of sediment metal background concentrations and enrichment in marine environments–a critical review, Sci. Total Environ. 580 (2017) 813–831.
[4] E. Ramirez-Llodra, A. Brandt, R. Danovaro, B. De Mol, E. Escobar, C.R. German, et al., Deep, diverse and definitely different: unique attributes of the world's largest ecosystem, Biogeosciences 7 (9) (2010) 2851–2899.
[5] W.-S. Shu, L.-N. Huang, Microbial diversity in extreme environments, Nat. Rev. Microbiol. 20 (4) (2022) 219–235.
[6] D. Zeppilli, D. Leduc, C. Fontanier, D. Fontaneto, S. Fuchs, A.J. Gooday, et al., Characteristics of meiofauna in extreme marine ecosystems: a review, Mar. Biodivers. 48 (2018) 35–71.
[7] C.R. Fisher, K. Takai, N. Le Bris, Hydrothermal vent ecosystems, Oceanography 20 (1) (2007) 14–23.
[8] E. Suess, Marine cold seeps and their manifestations: geological control, biogeochemical criteria and environmental conditions, Int. J. Earth Sci. 103 (2014) 1889–1916.
[9] A. Vanreusel, A.C. AndERSEN, A. BoETIUS, D. Connelly, M.R. Cunha, C. Decker, et al., Biodiversity of cold seep ecosystems along the European margins, Oceanography 22 (1) (2009) 110–127.
[10] R. Gibson, R. Atkinson, J. Gordon, Ecology of cold seep sediments: interactions of fauna with flow, chemistry and microbes, Oceanogr. Mar. Biol. Annu. Rev. 43 (2005) 1–46.
[11] E.K. Åström, A. Sen, M.L. Carroll, J. Carroll, Cold seeps in a warming Arctic: insights for benthic ecology, Front. Mar. Sci. 7 (2020) 244.
[12] V. Orphan, K.-U. Hinrichs, I.I.I.W. Ussler, C.K. Paull, L. Taylor, S.P. Sylva, et al., Comparative analysis of methane-oxidizing archaea and sulfate-reducing bacteria in anoxic marine sediments, Appl. Environ. Microbiol. 67 (4) (2001) 1922–1934.
[13] C.L. Zhang, Y. Li, J.D. Wall, L. Larsen, R. Sassen, Y. Huang, et al., Lipid and carbon isotopic evidence of methane-oxidizing and sulfate-reducing bacteria in association with gas hydrates from the Gulf of Mexico, Geology 30 (3) (2002) 239–242.
[14] E.O. Omoregie, H. Niemann, V. Mastalerz, G.J. de Lange, A. Stadnitskaia, J. Mascle, et al., Microbial methane oxidation and sulfate reduction at cold seeps of the deep Eastern Mediterranean Sea, Mar. Geol. 261 (1–4) (2009) 114–127.
[15] A. Boetius, M. Elvert, V. Samarkin, S.B. Joye, Molecular biogeochemistry of sulfate reduction, methanogenesis and the anaerobic oxidation of methane at Gulf of Mexico cold seeps, Geochem. Cosmochim. Acta 69 (17) (2005) 4267–4281.
[16] S.B. Joye, A. Boetius, B.N. Orcutt, J.P. Montoya, H.N. Schulz, M.J. Erickson, S.K. Lugo, The anaerobic oxidation of methane and sulfate reduction in sediments from Gulf of Mexico cold seeps, Chem. Geol. 205 (3–4) (2004) 219–238.
[17] D. Fornari, T. Shank, K. Von Damm, T. Gregg, M. Lilley, G. Levai, et al., Time-series temperature measurements at high-temperature hydrothermal vents, East Pacific Rise 9 49′–51′ N: evidence for monitoring a crustal cracking event, Earth Planet Sci. Lett. 160 (3–4) (1998) 419–431.
[18] Y. Li, K. Tang, L. Zhang, Z. Zhao, X. Xie, C.-T.A. Chen, et al., Coupled carbon, sulfur, and nitrogen cycles mediated by microorganisms in the water column of a shallow-water hydrothermal ecosystem, Front. Microbiol. 9 (2018) 2718.
[19] B. Jelen, D. Giovannelli, P.G. Falkowski, C. Vetriani, Elemental sulfur reduction in the deep-sea vent thermophile, Thermovibrio ammonificans, Environ. Microbiol. 20 (6) (2018) 2301–2316.
[20] P. Cruaud, A. Vigneron, P. Pignet, J.-C. Caprais, F. Lesongeur, L. Toffin, et al., Comparative study of Guaymas Basin microbiomes: cold seeps vs. hydrothermal vents sediments, Front. Mar. Sci. 4 (2017) 417.
[21] M. Portail, K. Olu, S.F. Dubois, E. Escobar-Briones, Y. Gelinas, L. Menot, J. Sarrazin, Food-web complexity in Guaymas Basin hydrothermal vents and cold seeps, PLoS One 11 (9) (2016) e0162263.
[22] S.E. Ruff, J.F. Biddle, A.P. Teske, K. Knittel, A. Boetius, A. Ramette, Global dispersion and local diversification of the methane seep microbiome, Proc. Natl. Acad. Sci. USA 112 (13) (2015) 4015–4020.
[23] B.N. Orcutt, J.B. Sylvan, N.J. Knab, K.J. Edwards, Microbial ecology of the dark ocean above, at, and below the seafloor, Microbiol. Mol. Biol. Rev. 75 (2) (2011) 361–422.
[24] Y. Wu, Y. Cao, C. Wang, M. Wu, O. Aharon, X. Xu, Microbial community structure and nitrogenase gene diversity of sediment from a deep-sea hydrothermal vent field on the Southwest Indian Ridge, Acta Oceanol. Sin. 33 (2014) 94–104.
[25] W.D. Orsi, Ecology and evolution of seafloor and subseafloor microbial communities, Nat. Rev. Microbiol. 16 (11) (2018) 671–683.
[26] H. Jing, R. Wang, Q. Jiang, Y. Zhang, X. Peng, Anaerobic methane oxidation coupled to denitrification is an important potential methane sink in deep-sea cold seeps, Sci. Total Environ. 748 (2020) 142459.
[27] M. Turnipseed, K. Knick, R. Lipcius, J. Dreyer, Dover C. Van, Diversity in mussel beds at deep-sea hydrothermal vents and cold seeps, Ecol. Lett. 6 (6) (2003) 518–523.
[28] H. Niemann, T. Lösekann, D. De Beer, M. Elvert, T. Nadalig, K. Knittel, et al., Novel microbial communities of the Haakon Mosby mud volcano and their role as a methane sink, Nature 443 (7113) (2006) 854–858.
[29] S. Yang, Y. Lv, X. Liu, Y. Wang, Q. Fan, Z. Yang, et al., Genomic and enzymatic evidence of acetogenesis by anaerobic methanotrophic archaea, Nat. Commun. 11 (1) (2020) 3941.
[30] T.M. McCollom, E.L. Shock, Geochemical constraints on chemolithoautotrophic metabolism by microorganisms in seafloor hydrothermal systems, Geochem. Cosmochim. Acta 61 (20) (1997) 4375–4391.
[31] G.J. Dick, The microbiomes of deep-sea hydrothermal vents: distributed globally, shaped locally, Nat. Rev. Microbiol. 17 (5) (2019) 271–283.
[32] J.-L. Birrien, X. Zeng, M. Jebbar, M.-A. Cambon-Bonavita, J. Quérellou, P. Oger, et al., Pyrococcus yayanosii sp. nov., an obligate piezophilic hyperthermophilic archaeon isolated from a deep-sea hydrothermal vent, Int. J. Syst. Evol. Microbiol. 61 (12) (2011) 2827–2881.
[33] X. Dong, C. Zhang, Y. Peng, H.-X. Zhang, L.-D. Shi, G. Wei, et al., Phylogenetically and catabolically diverse diazotrophs reside in deep-sea cold seep sediments, Nat. Commun. 13 (1) (2022) 4885.
[34] Q. Jiang, H. Jing, Q. Jiang, Y. Zhang, Insights into carbon-fixation pathways through metagonomics in the sediments of deep-sea cold seeps, Mar. Pollut. Bull. 176 (2022) 113458.
[35] M.P. Mehta, J.A. Baross, Nitrogen fixation at 92 C by a hydrothermal vent archaeon, Science 314 (5806) (2006) 1783–1786.
[36] T. Hoshino, H. Doi, G.-I. Uramoto, L. Wörmer, R.R. Adhikari, N. Xiao, et al., Global diversity of microbial communities in marine sediment, Proc. Natl. Acad. Sci. USA 117 (44) (2020) 27587–27597.
[37] J. Kennedy, J.R. Marchesi, A.D. Dobson, Marine metagenomics: strategies for the discovery of novel enzymes with biotechnological applications from marine environments, Microb. Cell Factories 7 (1) (2008) 1–8.
[38] F. Gründger, V. Carrier, M.M. Svenning, G. Panieri, T.R. Vonnahme, S. Klasek, H. Niemann, Methane-fuelled biofilms predominantly composed of methanotrophic ANME-1 in Arctic gas hydrate-related sediments, Sci. Rep. 9 (1) (2019) 9725.
[39] F. Bastida, D.J. Eldridge, C. García, G. Kenny Png, R.D. Bardgett, M. Delgado-Baquerizo, Soil microbial diversity–biomass relationships are driven by soil carbon content across global biomes, ISME J. 15 (7) (2021) 2081–2091.
[40] T. Dai, D. Wen, C.T. Bates, L. Wu, X. Guo, S. Liu, et al., Nutrient supply controls the linkage between species abundance and ecological interactions in marine bacterial communities, Nat. Commun. 13 (1) (2022) 175.
[41] G. Yvon-Durocher, A.P. Allen, D. Bastviken, R. Conrad, C. Gudasz, A. St-Pierre, et al., Methane fluxes show consistent temperature dependence across microbial to ecosystem scales, Nature 507 (7493) (2014) 488–491.
[42] E. Frouin, A. Lecoeuvre, F. Armougom, M.O. Schrenk, G. Erauso, Comparative metagenomics highlight a widespread pathway involved in catabolism of phosphonates in marine and terrestrial serpentinizing ecosystems, mSystems 7 (4) (2022) e00328, 22.

[43] X. Zhang, K. Wu, Z. Han, Z. Chen, Z. Liu, Z. Sun, et al., Microbial diversity and biogeochemical cycling potential in deep-sea sediments associated with seamount, trench, and cold seep ecosystems, Front. Microbiol. 13 (2022) 1029564.
[44] L.L. Demina, S.V. Galkin, Factors controlling the trace metal distribution in hydrothermal vent organisms, Trace Metal Biogeochemistry and Ecology of Deep-Sea Hydrothermal Vent Systems (2016) 123–141.
[45] S.B. Joye, M.W. Bowles, K. Ziervogel, Marine biogeochemical cycles, The Marine Microbiome (2022) 623–671.
[46] R. Herbert, Nitrogen cycling in coastal marine ecosystems, FEMS Microbiol. Rev. 23 (5) (1999) 563–590.
[47] E.E. Rios-Del Toro, E.I. Valenzuela, N.E. López-Lozano, M.G. Cortés-Martínez, M.A. Sánchez-Rodríguez, O. Calvario-Martínez, et al., Anaerobic ammonium oxidation linked to sulfate and ferric iron reduction fuels nitrogen loss in marine sediments, Biodegradation 29 (2018) 429–442.
[48] K. Wasmund, M. Mußmann, A. Loy, The life sulfuric: microbial ecology of sulfur cycling in marine sediments, Environmental microbiology reports 9 (4) (2017) 323–344.
[49] S. Begmatov, A.S. Savvichev, V.V. Kadnikov, A.V. Beletsky, I.I. Rusanov, A.A. Klyuvitkin, et al., Microbial communities involved in methane, sulfur, and nitrogen cycling in the sediments of the Barents Sea, Microorganisms 9 (11) (2021) 2362.
[50] Y. Liu, Z. Zhang, M. Ji, A. Hu, J. Wang, H. Jing, et al., Comparison of prokaryotes between mount everest and the mariana trench, Microbiome 10 (1) (2022) 215.
[51] V.P. Natarajan, X. Zhang, Y. Morono, F. Inagaki, F. Wang, A modified SDS-based DNA extraction method for high quality environmental DNA from seafloor environments, Front. Microbiol. 7 (2016) 986.
[52] Y. Chen, Y. Chen, C. Shi, Z. Huang, Y. Zhang, S. Li, et al., SOAPnuke: a MapReduce acceleration-supported software for integrated quality control and preprocessing of high-throughput sequencing data, GigaScience 7 (1) (2018) 1–6, https://doi.org/10.1093/gigascience/gix120.
[53] D. Li, R. Luo, C.M. Liu, C.M. Leung, H.F. Ting, K. Sadakane, et al., MEGAHIT v1.0: a fast and scalable metagenome assembler driven by advanced methodologies and community practices, Methods 102 (2016) 3–11, https://doi.org/10.1016/j.ymeth.2016.02.020.
[54] G.V. Uritskiy, J. DiRuggiero, J. Taylor, MetaWRAP—a flexible pipeline for genome-resolved metagenomic data analysis, Microbiome 6 (1) (2018), https://doi.org/10.1186/s40168-018-0541-1.
[55] M.R. Olm, C.T. Brown, B. Brooks, J.F. Banfield, dRep: a tool for fast and accurate genomic comparisons that enables improved genome recovery from metagenomes through de-replication, ISME J. 11 (12) (2017) 2864–2868, https://doi.org/10.1038/ismej.2017.126.
[56] P.-A. Chaumeil, A.J. Mussig, P. Hugenholtz, D.H. Parks, J. Hancock, GTDB-Tk: a toolkit to classify genomes with the Genome Taxonomy Database, Bioinformatics 36 (6) (2020) 1925–1927, https://doi.org/10.1093/bioinformatics/btz848.
[57] B. Langmead, S.L. Salzberg, Fast gapped-read alignment with Bowtie 2, Nat. Methods 9 (4) (2012) 357–359, https://doi.org/10.1038/nmeth.1923.
[58] D.H. Parks, M. Imelfort, C.T. Skennerton, P. Hugenholtz, G.W. Tyson, CheckM: assessing the quality of microbial genomes recovered from isolates, single cells, and metagenomes, Genome Res. 25 (7) (2015) 1043–1055, https://doi.org/10.1101/gr.186072.114.
[59] S. Capella-Gutiérrez, J.M. Silla-Martínez, T. Gabaldón, trimAl: a tool for automated alignment trimming in large-scale phylogenetic analyses, Bioinformatics 25 (15) (2009) 1972–1973, https://doi.org/10.1093/bioinformatics/btp348.
[60] L.-T. Nguyen, H.A. Schmidt, A. von Haeseler, B.Q. Minh, IQ-TREE: a fast and effective stochastic algorithm for estimating maximum-likelihood phylogenies, Mol. Biol. Evol. 32 (1) (2015) 268–274, https://doi.org/10.1093/molbev/msu300.
[61] M. Bastian, S. Heymann, M. Jacomy, Gephi: an open source software for exploring and manipulating networks, Proceedings of the International AAAI Conference on Web and Social Media 3 (1) (2009) 361–362, https://doi.org/10.1609/icwsm.v3i1.13937.
[62] D. Hyatt, G.-L. Chen, P.F. LoCascio, M.L. Land, F.W. Larimer, L.J. Hauser, Prodigal: prokaryotic gene recognition and translation initiation site identification, BMC Bioinf. 11 (1) (2010), https://doi.org/10.1186/1471-2105-11-119.
[63] L. Fu, B. Niu, Z. Zhu, S. Wu, W. Li, CD-HIT: accelerated for clustering the next-generation sequencing data, Bioinformatics 28 (23) (2012) 3150–3152, https://doi.org/10.1093/bioinformatics/bts565.
[64] T. Aramaki, R. Blanc-Mathieu, H. Endo, K. Ohkubo, M. Kanehisa, S. Goto, et al., KofamKOALA: KEGG Ortholog assignment based on profile HMM and adaptive score threshold, Bioinformatics 36 (7) (2020) 2251–2252, https://doi.org/10.1093/bioinformatics/btz859.